PLOS ONE

RESEARCH ARTICLE

Stimulus-induced narrow-band gamma oscillations in humans can be recorded using open-hardware low-cost EEG amplifier

Srividya Pattisapu, Supratim Ray*

Centre for Neuroscience, Indian Institute of Science, Bengaluru, India

* sray@iisc.ac.in

OPEN ACCESS

Citation: Pattisapu S, Ray S (2023) Stimulus-induced narrow-band gamma oscillations in humans can be recorded using open-hardware low-cost EEG amplifier. PLoS ONE 18(1): e0279881. https://doi.org/10.1371/journal.pone.0279881

Editor: Saeed Mian Qaisar, Effat University, SAUDI ARABIA

Received: December 11, 2021

Accepted: December 17, 2022

Published: January 23, 2023

Data Availability Statement: The data used in this study has been made publicly available and can be found at https://github.com/FlyingFordAnglia/OpenBCIGammaProject.

Funding: This work was supported by Wellcome Trust/DBT India Alliance (Senior fellowship IA/S/18/2/504003 to S.R.), and DBT-IISc Partnership Programme. The funders had no role in study design, data collection and analysis, decision to publish, or preparation of the manuscript.

Abstract

Stimulus-induced narrow-band gamma oscillations (30–70 Hz) in human electro-encephalograph (EEG) have been linked to attentional and memory mechanisms and are abnormal in mental health conditions such as autism, schizophrenia and Alzheimer's Disease. However, since the absolute power in EEG decreases rapidly with increasing frequency following a "1/f" power law, and the gamma band includes line noise frequency, these oscillations are highly susceptible to instrument noise. Previous studies that recorded stimulus-induced gamma oscillations used expensive research-grade EEG amplifiers to address this issue. While low-cost EEG amplifiers have become popular in Brain Computer Interface applications that mainly rely on low-frequency oscillations (< 30 Hz) or steady-state-visually-evoked-potentials, whether they can also be used to measure stimulus-induced gamma oscillations is unknown. We recorded EEG signals using a low-cost, open-source amplifier (OpenBCI) and a traditional, research-grade amplifier (Brain Products GmbH), both connected to the OpenBCI cap, in male (N = 6) and female (N = 5) subjects (22–29 years) while they viewed full-screen static gratings that are known to induce two distinct gamma oscillations: slow and fast gamma, in a subset of subjects. While the EEG signals from OpenBCI were considerably noisier, we found that out of the seven subjects who showed a gamma response in Brain Products recordings, six showed a gamma response in OpenBCI as well. In spite of the noise in the OpenBCI setup, the spectral and temporal profiles of these responses in alpha (8–13 Hz) and gamma bands were highly correlated between OpenBCI and Brain Products recordings. These results suggest that low-cost amplifiers can potentially be used in stimulus-induced gamma response detection.

Introduction

Gamma rhythms are narrow-band oscillations in the 30–70 Hz range of the brain's electrical activity [1]. They are associated with higher cognitive processes like attention [2–4], working memory [5] and feature binding [6], and are also found to be abnormal in mental health conditions like schizophrenia [7,8], autism [9] and Alzheimer's Disease (AD) [10]. Gamma oscillations can be induced in the occipital region of the brain when appropriate visual stimuli such

Competing interests: The authors have declared that no competing interests exist.

as bars and gratings are presented to the subjects [11,12], and such stimulus-induced gamma oscillations have been shown to decrease with healthy ageing [13] and with onset of AD [14]. Further, some studies have suggested a neuroprotective effect of entraining brain oscillations in the gamma range using sensory stimuli in rodent models of AD [15–17].

Recording gamma oscillations using EEG is fraught with difficulty. Cranial muscle activity from the scalp electrodes, high voltage activity from distant muscles such as the neck, and ocular muscular activity in the form of microsaccades can cause EEG artefacts in the gamma range [18–20]. One solution is to use Magnetoencephalogram (MEG), which has been shown to better capture gamma oscillations as compared to EEG [21,22], although such recording setups are bulky and expensive. Further, power of MEG/EEG signals falls rapidly with frequency, following a "1/f" power-law distribution [23]. Therefore, higher frequencies have much lower absolute power and are more susceptible to instrument noise. Mains (line) noise (50 or 60 Hz depending on the local power-line frequency) also lies within the gamma range. These factors make detection of gamma band oscillations using EEG difficult. These issues can be partially addressed by using research-grade amplifiers which have low input referred noise (noise generated by the internal circuitry of the amplifier in the absence of signals), high Common Mode Rejection Ratio (which amplifies the differential voltage while attenuating the common voltage between the positive and negative inputs), high input impedance to minimise the effect of high electrode impedance, and proper shielding of the electrical components of the amplifiers to reduce electromagnetic interference [24]. However, such amplifiers are generally bulky, expensive and often require proprietary software for usage. Several low-cost EEG acquisition systems have been developed in recent years (e.g. Emotiv (Emotiv Inc., San Francisco, California, U.S.A), NeuroSky TGAM, OpenBCI (OpenBCI, Inc., Brooklyn, New York, USA, www.openbci.com)), and their signal quality and performance has been studied in various contexts such as P-300 spelling task [25,26], Motor imagery based BCI paradigm [27], drowsiness detection [28], motor tasks [29] and Steady State Visually Evoked Potentials (SSVEP) [30]. However, these studies involve assessment of signals present at frequencies lower than 40Hz. To the best of our knowledge, no study has tested whether stimulus-induced narrowband gamma rhythms can be detected using low-cost EEG amplifier systems.

We assessed the performance of OpenBCI, a popular affordable amplifier which provides a good cost-effectiveness [31], in the detection of gamma rhythms when static full-field gratings known to elicit gamma rhythms [12] were presented to healthy human subjects. OpenBCI recordings were compared to the recordings obtained using Brain Products GmbH, a popular research-grade amplifier, under identical experimental conditions on the same subjects. The same electrode cap, stimulus presentation software, and downstream analyses were used in both cases so that any difference was attributable only to the amplifiers. Full-screen gratings induce two distinct bands in the gamma range [12], termed slow gamma (20–34 Hz) and fast gamma (35–66 Hz) bands, which have characteristic spectral and temporal profiles [32]. Therefore, in addition to comparing the amplitude of change in band powers between stimulus and baseline, we also compared the spectral pattern and temporal evolution of the gamma bands between the two recording systems. In addition to the gamma bands, we also compared the alpha band (8–13 Hz) power and temporal profiles.

Methods

Subjects

Eleven human subjects (6 males, 5 females, aged between 22–29 years) were recruited from the student community of the Indian Institute of Science, Bengaluru for the study on a voluntary basis against monetary compensation. Informed consent was obtained from all the subjects

prior to performing the experiment. All procedures were approved by the Institute Human Ethics Committee of the Indian Institute of Science.

Data acquisition

For every subject, EEG signals were recorded using two amplifiers: BrainAmp DC EEG acquisition system (Brain Products GmbH, Gilching, Germany) and OpenBCI Cyton Biosensing Board. For proper comparison, both were connected to the same electrode cap, OpenBCI EEG Electrode Cap, a 21-channel setup with sintered Ag/AgCl electrodes (https://docs.openbci.com/AddOns/Headwear/ElectrodeCap/). We used 8 of these passive, gel-based electrodes at the following locations using the internationally recognised 10–20 system [33]: O1, O2, P7, P3, Pz, P4, P8, CPz. During acquisition, the EEG signals were referenced to Cz (unipolar reference scheme [34]). If the impedance of any electrode exceeded 25 kΩ, it was rejected offline during analysis.

In the Brain Products setup, raw signals were recorded at 5 kHz native sampling rate in AC coupled mode, filtered online between 0.016 Hz (passive R-C hardware filter) and 250 Hz (fifth-order low pass, Butterworth hardware filter) and digitised at 16-bit resolution (0.1 μV/bit). Next, following an automatically applied digital low-pass Butterworth filter of 112.5 Hz cut-off to prevent aliasing, the data was downsampled to 250 Hz. This signal processing pipeline was implemented using BrainVision Recorder (Version 1.20.0701, Brain Products GmbH, Gilching, Germany). OpenBCI offers only an 8-channel recording with the requisite 250 Hz sampling rate, using a Bluetooth transmitter. While 16 channels can be used with an add-on board (OpenBCI Daisy board), it reduces the sampling rate to 125 Hz, which is too low for gamma range. A Wi-Fi shield was available which offered a higher sampling rate without losing on the channel availability, but it was still in beta phase at the time of our study. A higher sampling rate with 16 channels was also possible if data were recorded directly to the SD card on the equipment, but we opted to use streaming via Bluetooth for monitoring the signals in real time. For the OpenBCI setup, raw signals were recorded using OpenBCI GUI (version 5.0.2). Internally, OpenBCI first samples the signal at 1024 kHz in DC coupled mode followed by an R-C low-pass hardware filter of 72kHz. The signal is then digitised at 24-bit resolution (0.002235 μV/bit) followed by noise-shaping and a digital, third-order, low-pass sinc filter as the anti-aliasing filter (https://www.ti.com/lit/ds/symlink/ads1299.pdf) before downsampling to our chosen sampling rate of 250Hz. It was observed during experimental setup that the OpenBCI system was sensitive to ambient mains noise, especially when the digital I/O pins were used to collect event marker data, and care had to be taken to prevent small perturbations from creating noise artefacts. The OpenBCI amplifier (whose wiring and electronics were open to the air) was placed inside a copper mesh (whose dimensions did not exceed 30 cm in any direction), grounded to the UPS ground socket, to serve as a Faraday cage, to reduce line noise during acquisition and make it comparable to the Brain Products setup, which was already an enclosed system (further encasing the Brain Products setup inside a copper mesh did not improve recording quality). The copper mesh of the OpenBCI system was small enough not to impede the portability of the system. Eye tracking (monocular, left eye) was done for ten out of eleven subjects using Eye-Link 1000 (SR Research, Ontario, Canada) sampled at 1 kHz.

Experimental setting and behavioural task

All subjects sat in a dark room facing a gamma-corrected LCD monitor (BenQ XL2411; dimensions: 20.92×11.77 inches; resolution: 1289×720 pixels; refresh rate: 100 Hz) with their head supported by a chin rest at a distance of 57 cm from the screen. The experiment was performed in two sessions for each subject, one with OpenBCI and one with Brain Products

(sequence chosen randomly) separated by a break for few minutes. Each session consisted of one minute of eye-open recording and one minute of eye-closed recording for measurement, followed by a visual fixation task. The entire experiment lasted for an average duration of 2.1 hours (minimum: 1.25 hours, maximum: 2.75 hours).

In the visual fixation task, each trial comprised of a 1 second fixation duration and 1 second stimulus duration, with a 1 second inter-trial interval. The stimuli presented were static, full-contrast, sinusoidal-luminance, achromatic gratings with a combination of one of the three spatial frequencies (1, 2 or 4 cycles per degree (cpd), calibrated to viewing distance) and one of the four orientations (0˚, 45˚, 90˚ or 135˚) and were displayed pseudorandomly using NIMH MonkeyLogic software (version 2.0.236 [35]). These stimulus parameters were chosen as they were previously shown to induce robust gamma [12]. Each of the two sessions consisted of an average of 298 ± 10 trials (mean ± SD), for the 12 stimulus types combined. Trials in which the eye tracker recorded an eye blink or a shift in eye position beyond a 5˚ fixation window during fixation period or stimulus period were rejected online by the stimulus presentation software. The event markers for each stimulus type were conveyed to the two EEG acquisition devices using National Instruments USB-6008 Multifunction I/O Device.

Artefact rejection

A fully automated artefact rejection pipeline was used (for more details, see [13,14]). Briefly, trials with deviation from the mean signal in either time or frequency domains by more than 6 standard deviations were labelled as outliers and rejected. Subsequently, data from electrodes with too many outliers (> 40%) was discarded. This resulted in a rejection of 21.4 ± 16.6% (mean ± SD) of trials for the OpenBCI session and 11.8 ± 7.2% of the trials for the Brain Products session (although more trials were rejected with OpenBCI, the difference was not significant when compared using two-tailed Mann-Whitney U test (p-val = 0.3). Finally, any electrode whose slope of the baseline power spectrum in the 56–84 Hz range was less than zero was rejected. This led to the rejection of 3 electrodes in 2 subjects, 1 electrode in 1 subject and no rejection in the remaining 8 subjects in OpenBCI recordings. In the Brain Products recordings, 2 electrodes were rejected in 1 subject, 1 electrode in 1 subject and no rejection in the remaining 9 subjects. If either of the electrodes of a bipolar pair (see below for details) was marked for rejection, the whole pair was removed from analysis.

EEG data analysis

All analyses were performed using bipolar referencing scheme. Every electrode was re-referenced offline to its neighbour, yielding 5 bipolar electrode pairs (P7-O1, P3-O1, CPz-Pz, P4-O2, P8-O2) from the 8 unipolar electrodes. The bipolar referencing scheme was chosen because it yielded less noisy time–frequency spectra and a stronger gamma-band response in most subjects compared to unipolar referencing, in conformity with previous studies [13,14]. All the data analysis was done using custom codes written in MATLAB (The Mathworks Inc., 2021, version 9.10.0 (R2021a)). Brain Products data extraction included the usage of the 'bva-io' plug-in of EEGLAB toolbox (v12.0.2.5b [36], RRID: SCR_007292). Voltage measurements in OpenBCI recordings were sign-flipped [26] and were corrected offline to match the Brain Products standard while plotting Event Related Potentials (ERPs). The mains noise component was selectively attenuated offline prior to spectral analysis as follows [37]. First, we divided the unsegmented raw data into 180-second segments that contain integer cycles of the mains noise frequency. For each segment, we identified the frequency with maximum power using Fast-Fourier Transform in the 40–60 Hz range (to account for minor variations in the line noise frequency). A pure sinusoidal wave of that frequency (generated using inverse-FFT

with the power of all other frequencies set to zero) was subtracted from the raw data to obtain the mains-noise-filtered data. Because the line noise component was notched out at high-frequency resolution, it was invisible in PSDs computed over short time segments. Linear detrending was done to the raw EEG signals to correct for slow drifts. Power Spectral Densities (PSDs) and the time–frequency spectra were computed using the multitaper method [38] with a single taper using the Chronux toolbox (http://chronux.org/, RRID:SCR_005547 [39]). With timepoint 0 marking the onset of stimulus, baseline period was chosen between -750 ms and 0 ms, and stimulus period was chosen between +250 ms and +1000 ms, yielding a frequency resolution of 1.33 Hz for the PSDs. The periods were chosen to avoid stimulus-onset related transients. Time–frequency power spectra were calculated using a moving window of size 250 ms and a step size of 25 ms, giving a frequency resolution of 4 Hz.

Change in Power between stimulus and baseline periods for a frequency band was calculated using the following equation:

$$\Delta Power = 10\left(\log 10\frac{ST(f)}{\sum_f BL(f)}\right)$$

$$10log_{10}\left(\frac{\sum_f ST(f)}{\sum_f BL(f)}\right)$$

where ST is the stimulus power spectrum and BL is the baseline power spectrum, both averaged within relevant frequency bins (f), across all analysed trials and electrodes. Band powers of a single electrode are susceptible to variation among different subjects. Hence, band powers were averaged across electrodes for a more reliable comparison among subjects. Band powers were specifically computed in three frequency bands, namely slow gamma (20–34 Hz), fast gamma (35–66 Hz), and alpha (8–13 Hz). We note that beta oscillations also fall in the slow gamma range described in this study. Beta oscillations, however, are shown to be prominent at rest and attenuate with voluntary movements [40]. This is in contrast to the slow gamma oscillations which are shown to be almost invisible at rest and increase in power with visual stimulation [12]. We therefore refer to the 20–34 Hz band as the slow gamma range in our study. Peak frequency of a particular band was defined as the frequency at which the change in band power was maximum within that particular band.

ERPs were corrected for DC shift by subtracting the mean of the signal from each trial. The cross-correlation between the OpenBCI and Brain Products traces was computed using the *xcorr* function in MATLAB. The time at which the maximum of the cross-correlation function was observed was taken as the latency.

Slope of the PSD plot

For slope calculation, the PSDs were fit with the following power law function [23]:

$$P = A.f^{(-\alpha)} + B$$

where P is the power and f is the frequency, while A (scaling function), B (noise floor), and α (slope) are free parameters. To avoid over-fitting, we set B as the power at max frequency (125 Hz). Subsequently, linear regression was done on the log of Power (after subtracting the noise-floor) to obtain an estimate of A and α. As in our previous paper [13], slopes were calculated specifically for the 16–34 Hz and 54–88 Hz ranges to avoid contamination by the alpha range bump and line noise artefact and its harmonics. It is worth noting that the 54–88 Hz range slope also reflects muscular electrical activity.

Correlation analyses

Similarity between OpenBCI and Brain Product recordings was quantified using the Spearman correlation of the data points between the two sessions. Although interpretation of correlation coefficients can be complicated [41], we used these analyses to be consistent with our previous paper in which we compared the consistency of gamma oscillations in two recordings taken a year apart from the same subjects [32]. For band powers, the data points were the change in band power between the stimulus and baseline averaged across electrodes (yielding one value per frequency band for each subject). For assessment of similarity of temporal evolution, the data points were the time series of the mean band power change obtained using time frequency spectra. However, a high correlation between OpenBCI and Brain Products traces may be confounded by the possibility that the spectral profile in response to visual stimulus is common to all subjects. A previous study suggests that spectral and temporal profiles are unique to subjects and different in different subjects [32]. To assert whether these correlations indeed represent subject-specific trends and not a general similarity of all traces, we further compared correlations between the two recordings of the same subject and between different subjects. Correlation measures between OpenBCI and Brain Product recordings of the same subject are termed 'self-pair' correlations, and between OpenBCI and Brain Product recordings of two different subjects are termed 'cross-pair' correlations.

Statistical analysis

Appropriate non-parametric tests (Mann Whitney U test (Wilcoxon rank sum test) [42], permutation test [43]) were used to interpret the findings. Mann Whitney test was used to compare if the slope of the PSD was significantly different between the two EEG system recordings. It was also used to see whether there was a significant difference in gamma band power between stimulus and baseline periods for each subject. For asserting the significance of Spearman correlation values, permutation test was used. This involved computing the Spearman correlation between two ordered variables, and then repeating this process after shuffling the order. This produced a distribution of correlation values centred around zero, using which a p-value for the original correlation obtained can be computed. 0.05 was used as the cut-off for significance of the p-values.

Results

Instrument noise

Before EEG recordings, we characterized the internal instrument noise characteristics by placing the recording electrodes, along with the reference and ground in a common conducting salt bath (dashed lines in Fig 1). The power spectral density (PSD) for OpenBCI recordings (red dashed lines) showed larger line noise at 50 Hz compared to Brain Products (blue dashed lines), and also exhibited three additional peaks at 14 Hz, 36 (50–14) Hz and 64 (50+14) Hz. These peaks are due to modulation of the mains noise, that occurs due to non-linear distortion during amplification. No such artefactual peaks were observed for the Brain Products system. Even after shielding the OpenBCI setup for EEG recordings (which reduced the noise peak at 50 Hz, see Methods for details), these three peaks could be observed for some subjects (as shown below). These results were obtained after shielding the OpenBCI setup with a small copper mesh (described in Methods above), without which the OpenBCI setup had a large amount of line noise.

Baseline PSDs and slopes are comparable

Next, we compared EEG recordings in the pre-stimulus baseline period. Fig 1A (solid lines) shows the mean PSD across all subjects after averaging across all trials and up to 5 bipolar

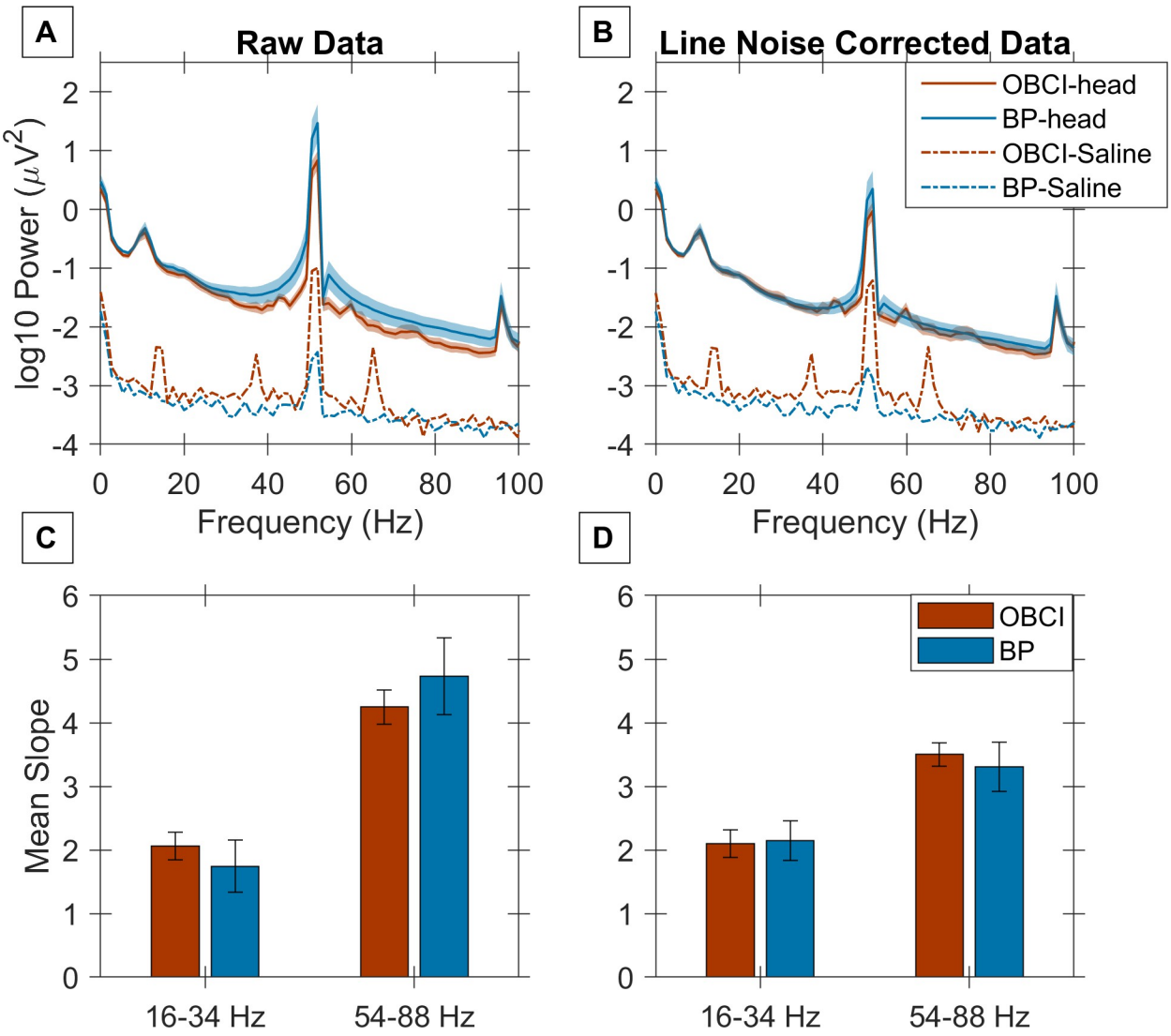

Fig 1. Slope comparison of OpenBCI and Brain Products at baseline. A) Baseline raw Power Spectral Density (PSD) for OpenBCI (*red trace*) and Brain Products (*blue trace*) averaged across 11 subjects (thickness of the trace indicates the standard error of PSD across subjects at each frequency). *Dotted lines* show PSD of shorted electrodes for instrument noise measurement. C) Slope of the PSD vs Frequency plot averaged across all subjects for two frequency ranges (16–34 Hz and 54–88 Hz) for OpenBCI (*red*) and Brain Products (*blue*). The error bars indicate the standard error. B, D) Same as A, C, but after selectively attenuating the mains/line noise component (see Methods for details).

https://doi.org/10.1371/journal.pone.0279881.g001

electrodes for each subject (see Methods for details). The Brain Products system had more mains noise than OpenBCI, possibly due to the usage of the Faraday shield for OpenBCI (no shield was used for Brain Products). To reduce the line noise artefact, we estimated the mains noise component in long segments of data and subtracted the same [37] before re-computing the PSD (see Methods for details), which yielded similar PSDs using both amplifiers (Fig 1B). We computed the slopes of the PSDs at two different frequency ranges: 16–34 Hz and 54–88 Hz, as per our previous report [13]. These ranges were chosen to prevent contamination due to the alpha band and line noise. These slopes were not significantly different between OpenBCI and Brain Products recordings (Fig 1C and 1D: raw-data: 16–34 Hz: $p = 0.69$, 54–88 Hz: $p = 0.33$, noise-corrected data: 16–34 Hz: $p = 0.90$; 54–88 Hz: $p = 0.74$; two-tailed Mann Whitney U test). The PSDs of the two systems were highly correlated (Spearman correlation

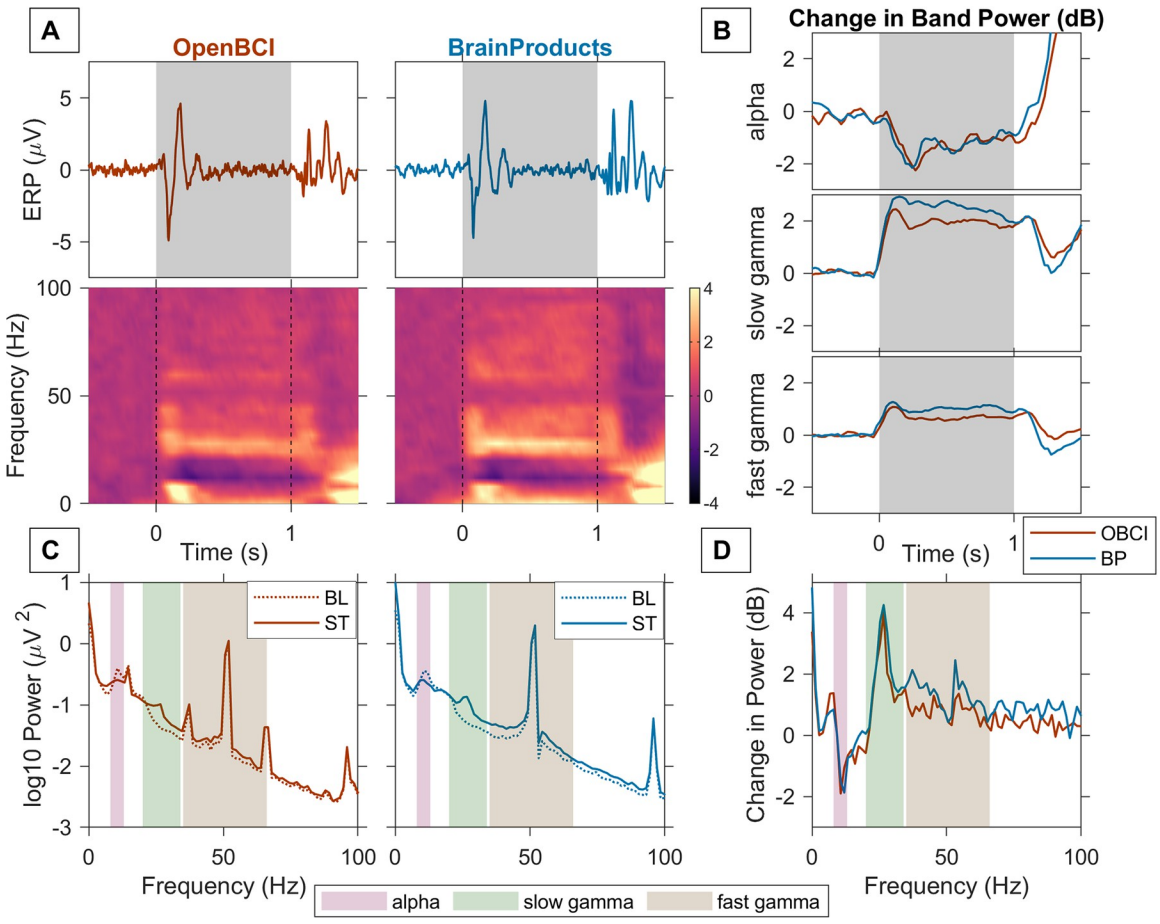

Fig 2. Stimulus induced gamma response in an example subject. A) Trial averaged EEG trace or ERP (*first row*) and time frequency spectrograms of change in power from baseline with time (*second row*). Vertical grey bars indicate stimulus duration (1 second). B) Change in Power (dB) from baseline as a function of time in alpha (8–13 Hz, *first row*), slow gamma (20–34 Hz, *second row*) and fast gamma (35–66 Hz, *third row*) bands recorded using OpenBCI (*red trace*) and Brain Products (*blue trace*). C) PSD for stimulus (*solid line*) and baseline (*dotted line*) averaged across 5 bipolar electrodes for OpenBCI (*left column*) and BrainProducts (*right column*). D) Change in power (dB) from baseline in stimulus period recorded using OpenBCI (*red trace*) and Brain Products (*blue trace*).

https://doi.org/10.1371/journal.pone.0279881.g002

coefficient of 0.91 for raw data ($p < 1e\text{-}06$, calculated using permutation test) and 0.93 for noise corrected data ($p < 1e\text{-}06$)). Interestingly, the first harmonic of noise was slightly lower than the expected 100 Hz in both setups. The reasons for this discrepancy are unclear. Note that the Brain Products setup was also much noisier than our previous EEG recordings done using the actiCap active electrodes provided by Brain Products (see, for example, comparable baseline PSDs in Fig 2 of Murty et al., 2020). As we discuss later, this is likely due to the use of the cheaper openBCI cap.

Fig 2 shows the results of an example subject (subject S2) for the visual fixation task. Trial and electrode averaged evoked potentials are plotted for OpenBCI (Fig 2A, left column) and Brain Products (Fig 2A, right column). These traces revealed a transient in the first 200 ms after stimulus onset and after the stimulus offset (i.e. after +1000ms). Change in power in stimulus period compared to baseline power revealed a prominent suppression in the alpha range and an increase in slow gamma power in both OpenBCI and Brain Products (Fig 2A, second row). The was also a broadband increase in power beyond the slow-gamma range, which was more prominent in Brain Products compared to OpenBCI. Power increase in the alpha band

after 1000ms of the trial was likely an eye blink or movement artefact during the inter-trial period. Fig 2C shows the PSD of the stimulus and baseline periods for the two amplifiers, demonstrating alpha (8–13 Hz) suppression and an increase in power in the slow-gamma (20–34 Hz) and the fast-gamma (35–66 Hz) bands, with the fast-gamma response being more appreciable in the Brain Products recording. Fig 2D shows the baseline subtracted PSDs for the two systems illustrating the same trend as above (since the log of PSD is subtracted, it is essentially a change in power from baseline, expressed in decibels). The change in power in alpha, slow and fast gamma bands as a function of time from their respective pre-stimulus baseline power is shown in Fig 2B. Overall, the increase in the band power is lower in OpenBCI than Brain Products for both the gamma bands, while it is similar for the alpha band (Fig 2A second row, 2B, 2C and 2D). Small noise peaks placed symmetrically around the mains noise band, indicating modulation distortions (also see Fig 1), can be observed in the PSDs of OpenBCI in this subject (Fig 2C, first column). However, since this noise is present in both pre-stimulus baseline period and stimulus-period, it gets cancelled out when we compute the change in power from baseline (Fig 2C and 2D).

Spectral and temporal patterns show similarity

Fig 3 shows the results of the visual fixation task for all the subjects sorted by decreasing gamma power. Visually similar results were obtained in the baseline-subtracted time frequency spectra of OpenBCI (first column) and Brain Products (second column). The change in power from baseline during stimulus at each frequency (Fig 3, third column), and the change in mean band power (in dB) of alpha, slow gamma and fast gamma bands with time (Fig 3, 4th, 5th and 6th columns respectively) also showed visually similar trends. However, the amplitude of change in band power can be seen to be lower in OpenBCI than in Brain Products in most subjects for the gamma bands, in particular for the fast gamma band.

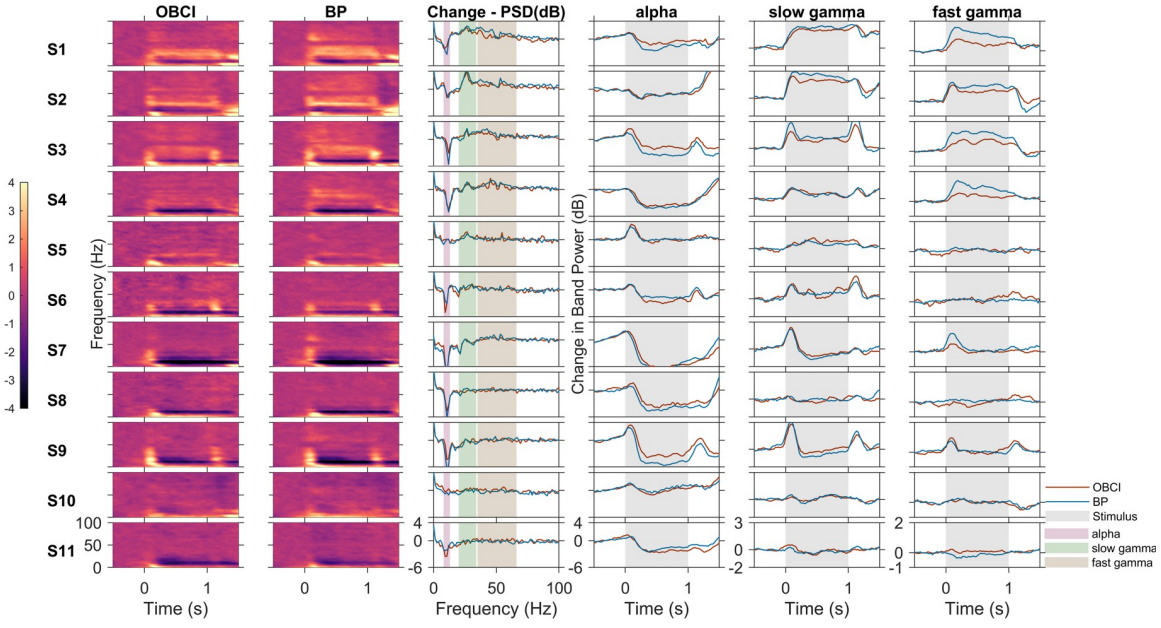

Fig 3. Comparison of OpenBCI and BrainProduct recordings for all subjects. Baseline subtracted time frequency spectrograms for OpenBCI (*first column* and *red trace* in other columns) and Brain Products (*second column* and *blue trace* in other columns), change in PSD (dB) from baseline in stimulus period vs frequency (*third column*), change in power (dB) with time for alpha (*fourth column*),slow gamma (*fifth column*) and fast gamma (*sixth column*) bands. Vertical bands in the last three columns indicate stimulus duration (*grey*). Each row represents one subject. The subjects are numbered in decreasing order of total gamma power.

https://doi.org/10.1371/journal.pone.0279881.g003

We considered a subject as having a "gamma response" if they showed a significant increase in band power between stimulus and baseline when compared across all analysable trials using one-tailed Mann-Whitney U test. False Discovery Rate (FDR) was controlled using the Benjamini and Hochberg procedure [44]. With this criterion, 6 subjects (S1 –S6) were found to have slow gamma response using both Brain Products and OpenBCI. For fast gamma, 5 subjects (S1 –S4,S7) showed a fast gamma response with Brain Products, out of which 4 subjects showed a fast gamma response (S1 –S4) with OpenBCI. A significant alpha suppression was observed in 10 subjects (all subjects except S5) using Brain Products and 9 subjects (all subjects except S5 and S10) using OpenBCI. In subject S10, while it is not apparent visually in Fig 3, there was a very small fast gamma increase (~ 0.1 dB increase from baseline in stimulus period) in OpenBCI recordings that was registered as significant by the statistical test we used, even after multiple testing correction. Similarly, alpha suppression in this subject was significant with Brain Products (but not OpenBCI), even though the suppression was small (~0.76 dB reduction from baseline in stimulus period). Overall, these results indicate that the power changes obtained using Brain Products and OpenBCI were highly consistent. To quantify these results, we computed the correlation between the change in band power from baseline in each frequency band of each subject using OpenBCI with that of Brain Products (Fig 4). The Spearman correlation coefficient for alpha band was 0.92 ($p < 1e\text{-}06$, computed using permutation test), for slow gamma was 0.94 ($p < 1e\text{-}06$) and for fast gamma was 0.75 ($p = 0.012$). For frequency wise correlation values across all subjects, see S1 Fig. The peak frequencies of the gamma bands were computed in those subjects who showed a gamma response, and in whom the gamma band had a clear peak instead of a broadband increase (specifically, in subjects S1-S6 in the slow gamma range). Four of these subjects showed an identical peak frequency between the two systems and the remaining two subjects showed a peak frequency within a difference of 2 Hz from each other. We compared this statistically using two-tailed Mann-Whitney U test and found no significant difference between the peak frequencies from the two systems ($p = 0.73$).

Amplitude of change in band powers appears to be better captured by Brain Products than OpenBCI

Although the correlation between power obtained using the two amplifiers was high, the distribution of points around the identity line (Fig 4) indicates that the amplitude of band power change was generally greater in Brain Products than OpenBCI. For alpha band, most points

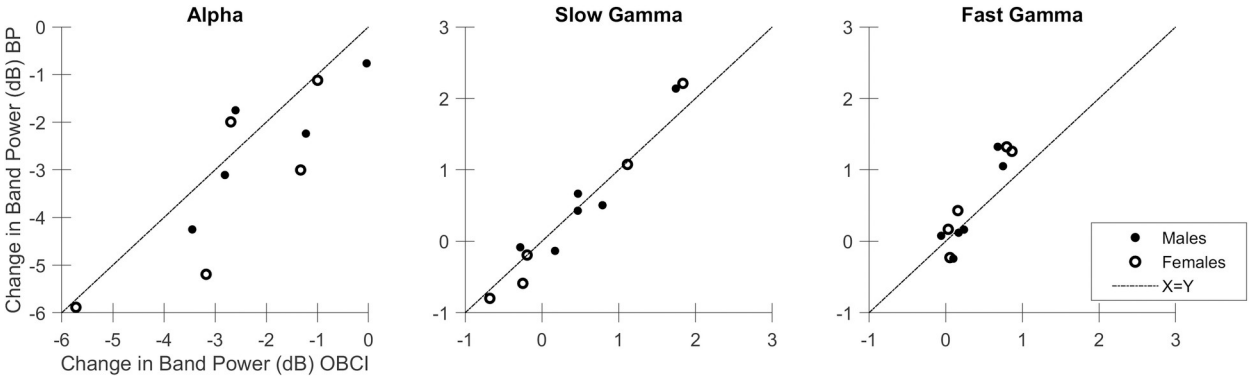

Fig 4. Comparison of change in Band Powers of OpenBCI and Brain Product recordings. Change in band power from baseline in stimulus period of alpha, slow gamma and fast gamma oscillations recorded using OpenBCI (*x axis*) and Brain Products (*y axis*) for males (*filled circles*) and females (*open circles*). *Dashed line* indicates identity line.

https://doi.org/10.1371/journal.pone.0279881.g004

lay below the identity line indicating that alpha suppression was better captured by Brain Products than OpenBCI. For fast gamma, the enhancement in gamma power was again better captured with Brain Products than OpenBCI, with the majority of data points above the identity line. For slow-gamma, the difference between the two devices appears less salient. However, note that the power in slow-gamma band is influenced by two opposing factors. First, there is an increase in power due to the slow-gamma rhythm, which is observed in about half of the subjects (S1 –S6). However, there is also a reduction in power in lower frequencies, which sometimes extended to the slow-gamma range. This is better observed in the subjects (S7 – S11) who did not have a strong slow-gamma rhythm, and their corresponding data points lay below zero dB in Fig 4 (middle panel). For those subjects, the points lay below the identity line, again reflecting better capture of low-frequency suppression by Brain Products than OpenBCI, and not poorer capture of the slow-gamma rhythm by Brain Products compared to OpenBCI.

ERPs are comparable but with a small delay

Fig 5 shows the de-trended and de-noised (see Methods for details) ERPs of OpenBCI and Brain Products for all subjects. A slight jitter can be seen in the OpenBCI traces compared to the Brain Products traces. Computing the cross-correlation between the two traces led to a median correlation (± standard error; computed using bootstrapping) of 0.79 ± 0.05, with OpenBCI traces lagging by 8 ± 0.5 milliseconds (cross-correlation value and the lag for each subject are indicated in the figure), corresponding to a lag of 2 sample points because our sampling frequency was 250 Hz. There was substantial variation in ERPs across subjects, consistent with our previous study where we show substantial variation in alpha and gamma responses across subjects which were nevertheless consistent across two recordings of the same subject [32],

Similarity between the two recordings within and between subjects

Next, we compared the temporal profile and the characteristic spectral distribution (see Introduction) between the two setups. The similarity of the change in band powers with time, and baseline subtracted PSDs of the two EEG amplifiers was quantified using Spearman correlation between the time series for each subject (see Methods). Self-pair correlations of baseline-subtracted PSD (0.51 ± 0.1, median ± standard error computed using bootstrapping) were significantly higher than its cross-pair correlations (0.33 ± 0.02, p = 1.07e-04, one sided Mann Whitney U test, Fig 6A). Similar results were obtained for the temporal evolution traces in alpha, slow gamma and fast gamma bands:(alpha: self: 0.93 ± 0.04; cross: 0.52 ± 0.07, p = 7.4e-6, Fig 6B; slow gamma: self: 0.82 ± 0.05; cross: 0.31 ± 0.06, p = 6.01e-06, Fig 6C; fast gamma: self: 0.68 ± 0.15, cross: 0.22 ± 0.04, p = 2.7e-4, Fig 6D). When self-pair correlations were plotted against cross-pair correlations, their values were concentrated below the identity line (Fig 6).

Discussion

Our study is the first one to assess the performance of a low-cost amplifier in the detection of stimulus induced gamma response and compare it with a research grade amplifier while controlling for subjects, electrodes and electrode placement, task performed and subsequent analysis. We showed that a low-cost EEG amplifier like OpenBCI is able to detect gamma response in subjects, and the spectral and temporal profiles from OpenBCI recordings are correlated to that of a research grade amplifier like Brain Products when full screen static gratings are presented as stimuli. Correlations between the two recordings of the same subjects ('self-pair correlations') were significantly higher than correlations between different subjects ('cross-pair

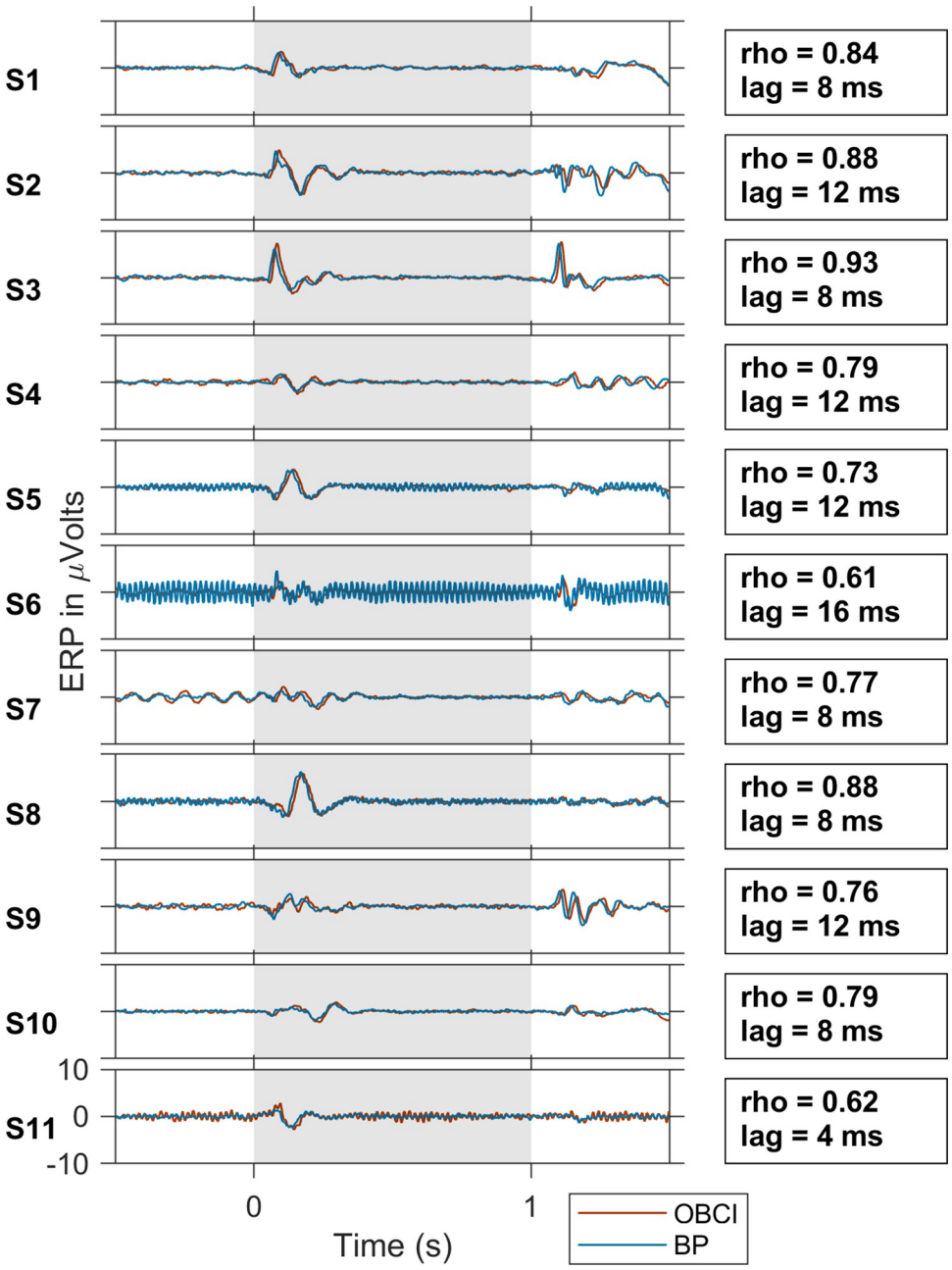

Fig 5. ERP Plots of all subjects. ERPs for OpenBCI (*red trace*) and Brain Products (*blue trace*) for all subjects. The subjects are numbered in decreasing order of gamma power, as in Fig 3. The *vertical grey* shaded region indicates the stimulus duration. The cross-correlation coefficient and lag between OpenBCI and Brain Products are indicated on the right for each subject.

https://doi.org/10.1371/journal.pone.0279881.g005

correlations') indicating that the distinctiveness in spectral and temporal profiles across different subjects could be captured by these amplifiers.

Although we were able to record gamma oscillations using OpenBCI, the overall performance of Brain Products was superior. There was lesser noise and fewer bad trials and electrodes in Brain Products recordings compared to OpenBCI. The change in power in the gamma band was of a lower amplitude in OpenBCI than Brain Products, especially in the fast

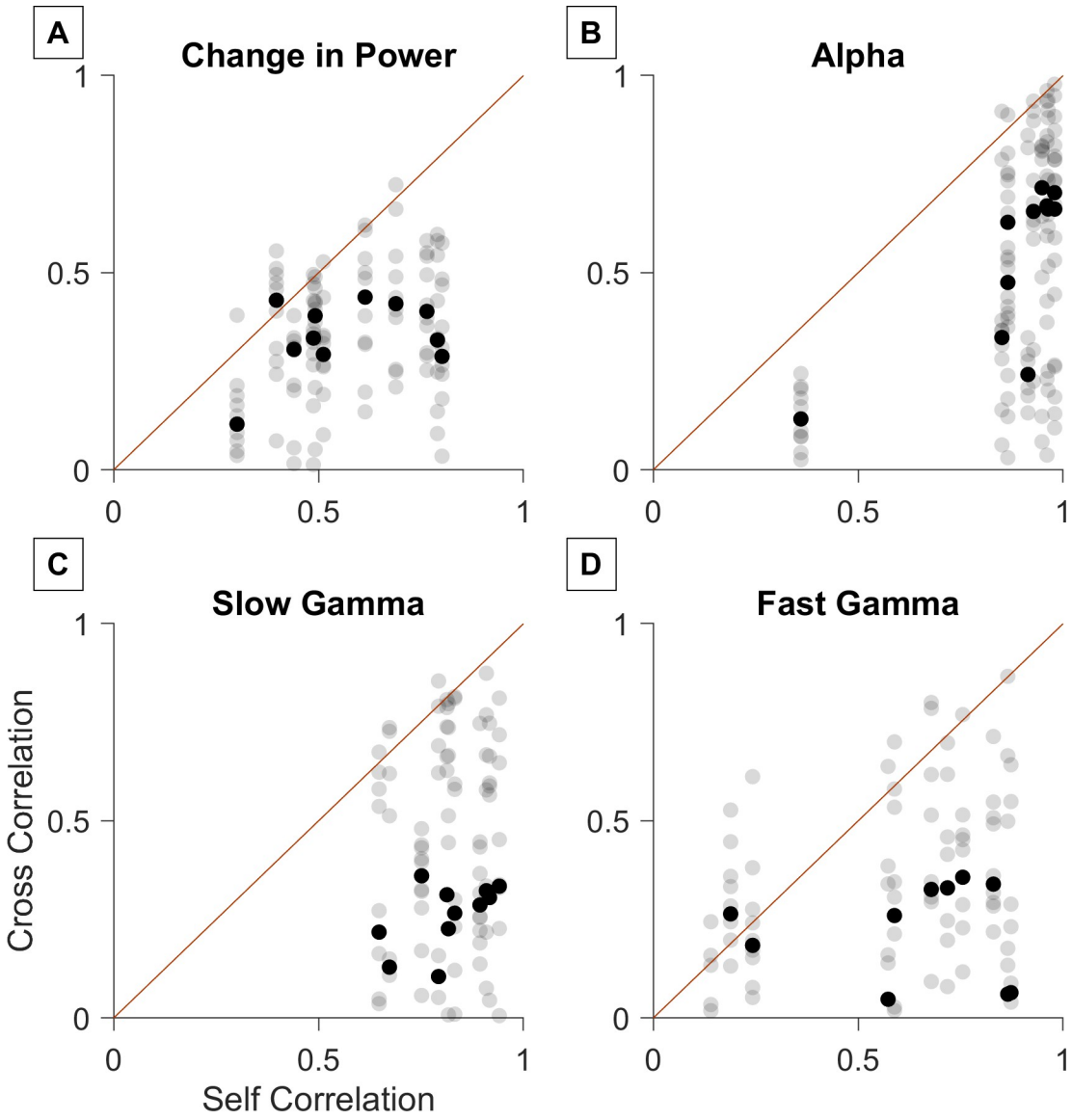

Fig 6. Comparison of self-pair correlations and cross-pair correlations. Self pair correlations (between OpenBCI and Brain Products recordings of same subjects) vs cross pair correlations (between OpenBCI and Brain Products recordings of different subjects) for change in PSD from baseline in stimulus period (A) and change in power with time for alpha (B), slow gamma (C) and fast gamma (D) bands. *Red line* indicates x = y line. The *bold black marker* indicates the median of the cross pair correlations for each subject.

https://doi.org/10.1371/journal.pone.0279881.g006

gamma band. We found that 7/11 subjects showed a gamma response (either fast or slow) with Brain Products (out of which 6/11 subjects showed a gamma response, either slow or fast, with OpenBCI), a fraction that is considerably lower than what was observed in a previous study in which more than 80% of subjects showed a gamma response with Brain Products recordings [13]. We interpret this finding with caution, since the sample size in this study was considerably lower than the previous study. The main difference in the Brain Products recordings between these two studies was that we used the OpenBCI cap with passive electrodes here, while we used ActiCap with active electrodes from Brain Products in the previous study. Much more work needs to be done to evaluate the clinical utility of EEG-derived gamma oscillations,

in particular to test if the fraction of subjects who show a gamma response can be increased by using different caps, or by employing source localization techniques to better isolate the gamma response (which may in turn depend on the number of sensors). Further, potential functional correlation with clinical signatures must be determined.

In addition, EEG-derived gamma responses need to be compared with comparable MEG recordings (with/without source localization), because EEG-derived gamma responses could be affected by muscle activity related to microsaccades and electromyographic activity from cranial and neck muscles even in tasks not requiring any muscle activity [18–20]. We note here that even though microsaccades have been shown to produce a signature in the EEG in the gamma band [19], it is clear that the slow and fast gamma responses described here have a distinct biophysical origin. First, in our previous studies [13,14], we rigorously analyzed the microsaccades by computing the main sequence [45], and showed that all results hold even when considering trials in which no microsaccades are detected. Second, stimulus-induced slow and fast gamma are sustained throughout the duration of the trial, while microsaccade induced gamma is transient. Further, slow gamma power typically increases over time while fast gamma power reduces over time [12], ruling out the possibility that both are artefacts of microsaccades. Finally, these stimulus-induced gamma oscillations are highly dependent on stimulus properties, and closely resemble the trends observed in animal studies [12] where eye movements are rigorously controlled.

Comparisons between low-cost and research-grade amplifiers in previous studies

Previous studies have assessed the performance of low-cost EEG amplifiers in various contexts. While some studies have only assessed the performance of a low-cost amplifier in the absence of a research grade control [27,46], others have compared their performance with a research grade amplifier but have not controlled for factors like the use of same electrodes, same subjects or downstream analysis to reliably attribute all differences only to the amplifiers [47,48]. de Vos and colleagues [25] compared the performance of an Emotiv based setup with Brain Products GmbH with the same electrodes in the context of a P300 spelling task in 13 subjects. However, they mainly compared the P300 ERP topographies and spelling task performance ($r > 0.77$), with no frequency domain comparison. In a study done by Frey, 2016 [26], OpenBCI signals were compared to the signals from g.tec g.USBamp amplifier (another research grade amplifier) from one subject in a P300 spelling task and a working memory load task. The study used a custom adapter which enabled simultaneous recording with two amplifiers using the same electrodes in the same recording session. The study reported a high correlation between ERPs and PSDs of the two amplifiers ($r > 0.99$). Their simultaneous recording from the two amplifiers in a single recording session as opposed to our sequential recording sessions and their low sample size ($n = 1$) could be an explanation for the lower ERP correlation values (mean $r = 0.79$) and PSD correlation values we found in our study during baseline period ($r = 0.93$). Also, their spectral analyses were restricted to frequencies < 40 Hz, which does not include the mains noise range, potentially contributing to a higher correlation value. They also reported a slight jitter (88 ms) in the ERP of OpenBCI compared to g.tec. While we have also found a small jitter in the ERP of OpenBCI (median lag = 8 ms, Fig 5) compared to Brain Products, we did not correct for it since all our analyses were in the frequency domain. Rashid et. al. [29] reported no significant difference in the power of signals between OpenBCI and NuAmps (another research grade amplifier) in the beta band (12–38 Hz, which includes slow gamma frequencies) in 22 participants, but the task performed was a motor task.

Comparison in performance of OpenBCI for different frequency bands

Previous studies have shown that in the presence of static, full-field visual gratings, two gamma bands are found in the EEG: a slow gamma band (20–34 Hz) and a fast gamma band (35–66 Hz) [12,13]. In addition, alpha band is also suppressed. In our study, slow gamma was found to be better retrieved by OpenBCI than fast gamma in terms of amplitude of change in band power and correlation of its temporal evolution (Figs 3 and 6). This could be due to the contamination of fast gamma with the cross-modulation noise bands (Fig 1, dashed lines and Fig 2C, left). Slow gamma and fast gamma bands were both found to be reduced in Alzheimer's disease and Mild Cognitive Impairment patients in a study done by Murty and colleagues [14]. Further, previous studies have shown that slow gamma band is more reliable with age than fast gamma [13] and shows more inter-subject variability and better test-retest reliability [32]. This raises the possibility of using OpenBCI to detect slow gamma as a biomarker or screening tool in low resource settings.

Conclusion

OpenBCI is a low-cost EEG amplifier whose open-hardware nature offers customisability and ease of interface with existing equipment, and its lack of bulk offers mobility which allows extensibility of experiments and usage in natural environments outside of dedicated laboratories. OpenBCI amplifier was noisier than Brain Products amplifier when both were connected to the OpenBCI cap. Further, signals from Brain Products were noisier than our previous studies when we used Brain Products ActiCaps instead of the OpenBCI cap, suggesting that part of the noise was due to the use of the OpenBCI cap. Nevertheless, OpenBCI was able to capture the gamma response in most of the subjects that showed a gamma response using Brain Products amplifier. Our study suggests that OpenBCI has potential as a low-cost alternative to traditional research grade amplifiers in the detection of stimulus induced gamma oscillations, although more research is needed to improve the signal quality and test its usefulness in clinical settings.

Supporting information

S1 Fig. Frequency wise Spearman correlation of power recorded using the two amplifiers across all subjects, plotted across frequency. *Black circles* are for correlation values whose p-values calculated with permutation test are more than 0.05 and *green circles* are for correlation values whose p-values are less than 0.05. False Discovery Rate of p-values is controlled using Benjamini and Hochberg (1995) procedure.
(TIF)

Author Contributions

Conceptualization: Srividya Pattisapu, Supratim Ray.

Data curation: Srividya Pattisapu.

Formal analysis: Srividya Pattisapu, Supratim Ray.

Funding acquisition: Supratim Ray.

Investigation: Srividya Pattisapu.

Methodology: Srividya Pattisapu.

Resources: Supratim Ray.

Supervision: Supratim Ray.

Visualization: Srividya Pattisapu.

Writing – original draft: Srividya Pattisapu.

Writing – review & editing: Srividya Pattisapu, Supratim Ray.

References

1. Buzsáki G, Wang XJ. Mechanisms of Gamma Oscillations. Annu Rev Neurosci [Internet]. 2012 [cited 2021 Sep 23]; 35:203–25. Available from: https://www.ncbi.nlm.nih.gov/pmc/articles/PMC4049541/. https://doi.org/10.1146/annurev-neuro-062111-150444 PMID: 22443509
2. Fries P. Modulation of Oscillatory Neuronal Synchronization by Selective Visual Attention. Science [Internet]. 2001 Feb 23 [cited 2021 Sep 27]; 291(5508):1560–3. Available from: https://www.sciencemag.org/lookup/doi/10.1126/science.1055465. PMID: 11222864
3. Gregoriou GG, Gotts SJ, Zhou H, Desimone R. High-Frequency, Long-Range Coupling Between Prefrontal and Visual Cortex During Attention. Science [Internet]. 2009 May 29 [cited 2021 Sep 27]; 324 (5931):1207–10. Available from: https://www.sciencemag.org/lookup/doi/10.1126/science.1171402. PMID: 19478185
4. Chalk M, Herrero JL, Gieselmann MA, Delicato LS, Gotthardt S, Thiele A. Attention Reduces Stimulus-Driven Gamma Frequency Oscillations and Spike Field Coherence in V1. Neuron [Internet]. 2010 Apr [cited 2021 Sep 27]; 66(1):114–25. Available from: https://linkinghub.elsevier.com/retrieve/pii/S0896627310001844. https://doi.org/10.1016/j.neuron.2010.03.013 PMID: 20399733
5. Pesaran B, Pezaris JS, Sahani M, Mitra PP, Andersen RA. Temporal structure in neuronal activity during working memory in macaque parietal cortex. Nat Neurosci [Internet]. 2002 Aug [cited 2021 Sep 27]; 5(8):805–11. Available from: http://www.nature.com/articles/nn890. https://doi.org/10.1038/nn890 PMID: 12134152
6. Gray CM, König P, Engel AK, Singer W. Oscillatory responses in cat visual cortex exhibit inter-columnar synchronization which reflects global stimulus properties. Nature [Internet]. 1989 Mar [cited 2021 Sep 27]; 338(6213):334–7. Available from: http://www.nature.com/articles/338334a0. https://doi.org/10.1038/338334a0 PMID: 2922061
7. Hirano Y, Oribe N, Kanba S, Onitsuka T, Nestor PG, Spencer KM. Spontaneous Gamma Activity in Schizophrenia. JAMA Psychiatry [Internet]. 2015 Aug 1 [cited 2021 Sep 27]; 72(8):813. Available from: http://archpsyc.jamanetwork.com/article.aspx?do=10.1001/jamapsychiatry.2014.2642i. PMID: 25587799
8. Tada M, Nagai T, Kirihara K, Koike S, Suga M, Araki T, et al. Differential Alterations of Auditory Gamma Oscillatory Responses Between Pre-Onset High-Risk Individuals and First-Episode Schizophrenia. Cereb Cortex [Internet]. 2016 Mar [cited 2021 Sep 27]; 26(3):1027–35. Available from: https://academic.oup.com/cercor/article-lookup/doi/10.1093/cercor/bhu278. PMID: 25452567
9. Kmin An, Ikeda T, Yoshimura Y, Hasegawa C, Saito DN, Kumazaki H, et al. Altered Gamma Oscillations during Motor Control in Children with Autism Spectrum Disorder. J Neurosci [Internet]. 2018 Sep 5 [cited 2021 Sep 27]; 38(36):7878–86. Available from: https://www.jneurosci.org/lookup/doi/10.1523/JNEUROSCI.1229-18.2018. PMID: 30104338
10. Verret L, Mann EO, Hang GB, Barth AMI, Cobos I, Ho K, et al. Inhibitory Interneuron Deficit Links Altered Network Activity and Cognitive Dysfunction in Alzheimer Model. Cell [Internet]. 2012 Apr 27 [cited 2021 Oct 7]; 149(3):708–21. Available from: https://www.cell.com/cell/abstract/S0092-8674(12)00284-X. https://doi.org/10.1016/j.cell.2012.02.046 PMID: 22541439
11. Jia X, Tanabe S, Kohn A. Gamma and the Coordination of Spiking Activity in Early Visual Cortex. Neuron [Internet]. 2013 Feb 20 [cited 2021 Oct 27]; 77(4):762–74. Available from: https://www.sciencedirect.com/science/article/pii/S0896627313000445.
12. Murty DVPS, Shirhatti V, Ravishankar P, Ray S. Large Visual Stimuli Induce Two Distinct Gamma Oscillations in Primate Visual Cortex. J Neurosci [Internet]. 2018 Mar 14 [cited 2021 Sep 19]; 38 (11):2730–44. Available from: https://www.jneurosci.org/lookup/doi/10.1523/JNEUROSCI.2270-17.2017. PMID: 29440388
13. Murty DVPS, Manikandan K, Kumar WS, Ramesh RG, Purokayastha S, Javali M, et al. Gamma oscillations weaken with age in healthy elderly in human EEG. NeuroImage [Internet]. 2020 Jul [cited 2021 Sep 19]; 215:116826. Available from: https://linkinghub.elsevier.com/retrieve/pii/S105381192030313X. https://doi.org/10.1016/j.neuroimage.2020.116826 PMID: 32276055
14. Murty DV, Manikandan K, Kumar WS, Ramesh RG, Purokayastha S, Nagendra B, et al. Stimulus-induced gamma rhythms are weaker in human elderly with mild cognitive impairment and Alzheimer's

disease. eLife [Internet]. 2021 Jun 8 [cited 2021 Sep 19]; 10:e61666. Available from: https://elifesciences.org/articles/61666. https://doi.org/10.7554/eLife.61666 PMID: 34099103

15. Adaikkan C, Middleton SJ, Marco A, Pao PC, Mathys H, Kim DNW, et al. Gamma Entrainment Binds Higher-Order Brain Regions and Offers Neuroprotection. Neuron [Internet]. 2019 Jun [cited 2021 Sep 27]; 102(5):929–943.e8. Available from: https://linkinghub.elsevier.com/retrieve/pii/S0896627319303460. https://doi.org/10.1016/j.neuron.2019.04.011 PMID: 31076275

16. Iaccarino HF, Singer AC, Martorell AJ, Rudenko A, Gao F, Gillingham TZ, et al. Gamma frequency entrainment attenuates amyloid load and modifies microglia. Nature [Internet]. 2016 Dec 8 [cited 2021 Sep 27]; 540(7632):230–5. Available from: http://www.nature.com/articles/nature20587. https://doi.org/10.1038/nature20587 PMID: 27929004

17. Martorell AJ, Paulson AL, Suk HJ, Abdurrob F, Drummond GT, Guan W, et al. Multi-sensory Gamma Stimulation Ameliorates Alzheimer's-Associated Pathology and Improves Cognition. Cell [Internet]. 2019 Apr [cited 2021 Sep 27]; 177(2):256–271.e22. Available from: https://linkinghub.elsevier.com/retrieve/pii/S0092867419301631. https://doi.org/10.1016/j.cell.2019.02.014 PMID: 30879788

18. Hipp J, Siegel M. Dissociating neuronal gamma-band activity from cranial and ocular muscle activity in EEG. Frontiers in Human Neuroscience [Internet]. 2013 [cited 2022 May 13];7. Available from: https://www.frontiersin.org/article/10.3389/fnhum.2013.00338. https://doi.org/10.3389/fnhum.2013.00338 PMID: 23847508

19. Yuval-Greenberg S, Tomer O, Keren AS, Nelken I, Deouell LY. Transient Induced Gamma-Band Response in EEG as a Manifestation of Miniature Saccades. Neuron [Internet]. 2008 May 8 [cited 2022 May 13]; 58(3):429–41. Available from: https://www.sciencedirect.com/science/article/pii/S0896627308003012. https://doi.org/10.1016/j.neuron.2008.03.027 PMID: 18466752

20. Whitham EM, Lewis T, Pope KJ, Fitzgibbon SP, Clark CR, Loveless S, et al. Thinking activates EMG in scalp electrical recordings. Clinical Neurophysiology [Internet]. 2008 May 1 [cited 2022 May 14]; 119(5):1166–75. Available from: https://www.sciencedirect.com/science/article/pii/S138824570800045X. https://doi.org/10.1016/j.clinph.2008.01.024 PMID: 18329954

21. Muthukumaraswamy SD, Singh KD. Visual gamma oscillations: the effects of stimulus type, visual field coverage and stimulus motion on MEG and EEG recordings. Neuroimage. 2013 Apr 1; 69:223–30. https://doi.org/10.1016/j.neuroimage.2012.12.038 PMID: 23274186

22. Orekhova EV, Butorina AV, Sysoeva OV, Prokofyev AO, Nikolaeva AYu, Stroganova TA. Frequency of gamma oscillations in humans is modulated by velocity of visual motion. Journal of Neurophysiology [Internet]. 2015 Jul [cited 2022 May 13]; 114(1):244–55. Available from: https://journals.physiology.org/doi/full/10.1152/jn.00232.2015.

23. Miller KJ, Sorensen LB, Ojemann JG, den Nijs M. Power-Law Scaling in the Brain Surface Electric Potential. Sporns O, editor. PLoS Comput Biol [Internet]. 2009 Dec 18 [cited 2021 Sep 19]; 5(12):e1000609. Available from: https://dx.plos.org/10.1371/journal.pcbi.1000609. https://doi.org/10.1371/journal.pcbi.1000609 PMID: 20019800

24. Usakli AB. Improvement of EEG Signal Acquisition: An Electrical Aspect for State of the Art of Front End. Computational Intelligence and Neuroscience [Internet]. 2010 Feb 2 [cited 2021 Oct 9]; 2010:e630649. Available from: https://www.hindawi.com/journals/cin/2010/630649/. https://doi.org/10.1155/2010/630649 PMID: 20148074

25. De Vos M, Kroesen M, Emkes R, Debener S. P300 speller BCI with a mobile EEG system: comparison to a traditional amplifier. J Neural Eng [Internet]. 2014 Jun 1 [cited 2021 Sep 28]; 11(3):036008. Available from: https://iopscience.iop.org/article/10.1088/1741-2560/11/3/036008. https://doi.org/10.1088/1741-2560/11/3/036008 PMID: 24763067

26. Frey J. Comparison of an open-hardware electroencephalography amplifier with medical grade device in brain-computer interface applications. arXiv:160602438 [cs] [Internet]. 2016 Jun 8 [cited 2021 Sep 27]; Available from: http://arxiv.org/abs/1606.02438.

27. Peterson V, Galván C, Hernández H, Spies R. A feasibility study of a complete low-cost consumer-grade brain-computer interface system. Heliyon [Internet]. 2020 Mar [cited 2021 Sep 27]; 6(3):e03425. Available from: https://linkinghub.elsevier.com/retrieve/pii/S240584402030270X. https://doi.org/10.1016/j.heliyon.2020.e03425 PMID: 32154404

28. LaRocco J, Le MD, Paeng DG. A Systemic Review of Available Low-Cost EEG Headsets Used for Drowsiness Detection. Front Neuroinform [Internet]. 2020 Oct 15 [cited 2021 Sep 27]; 14:553352. Available from: https://www.frontiersin.org/article/10.3389/fninf.2020.553352/full. https://doi.org/10.3389/fninf.2020.553352 PMID: 33178004

29. Rashid U, Niazi I, Signal N, Taylor D. An EEG Experimental Study Evaluating the Performance of Texas Instruments ADS1299. Sensors [Internet]. 2018 Nov 1 [cited 2021 Sep 27]; 18(11):3721. Available from: http://www.mdpi.com/1424-8220/18/11/3721. https://doi.org/10.3390/s18113721 PMID: 30388836

30. Sawangjai P, Hompoonsup S, Leelaarporn P, Kongwudhikunakorn S, Wilaiprasitporn T. Consumer Grade EEG Measuring Sensors as Research Tools: A Review. IEEE Sensors J [Internet]. 2020 Apr 15 [cited 2021 Oct 10]; 20(8):3996–4024. Available from: https://ieeexplore.ieee.org/document/8945233/.

31. Aldridge A, Barnes E,Bethel CL, Carruth DW, Kocturova M, Pleva M, et al. Accessible Electroencephalograms (EEGs): A Comparative Review with OpenBCI's Ultracortex Mark IV Headset. In: 2019 29th International Conference Radioelektronika (RADIOELEKTRONIKA) [Internet]. Pardubice, Czech Republic: IEEE; 2019 [cited 2021 Sep 27]. p. 1–6. Available from: https://ieeexplore.ieee.org/document/8733482/.

32. Kumar WS, Manikandan K, Murty DVPS, Ramesh RG, Purokayastha S, Javali M, et al. Stimulus-induced narrowband gamma oscillations are test-retest reliable in healthy elderly in human EEG. bioRxiv [Internet]. 2021; Available from: https://www.biorxiv.org/content/early/2021/07/09/2021.07.06.451226.

33. Silverman D. The Rationale and History of the 10–20 System of the International Federation. American Journal of EEG Technology [Internet]. 1963 Mar [cited 2021 Sep 28]; 3(1):17–22. Available from: https://www.tandfonline.com/doi/full/10.1080/00029238.1963.11080602.

34. Yao D, Qin Y, Hu S, Dong L, Bringas Vega ML, Valdés Sosa PA. Which Reference Should We Use for EEG and ERP practice? Brain Topogr [Internet]. 2019 Jul [cited 2021 Sep 28]; 32(4):530–49. Available from: http://link.springer.com/10.1007/s10548-019-00707-x. https://doi.org/10.1007/s10548-019-00707-x PMID: 31037477

35. Hwang J, Mitz AR, Murray EA. NIMH MonkeyLogic: Behavioral control and data acquisition in MATLAB. Journal of Neuroscience Methods [Internet]. 2019 Jul [cited 2021 Sep 28]; 323:13–21. Available from: https://linkinghub.elsevier.com/retrieve/pii/S0165027019301360. https://doi.org/10.1016/j.jneumeth.2019.05.002 PMID: 31071345

36. Delorme A, Makeig S. EEGLAB: an open source toolbox for analysis of single-trial EEG dynamics including independent component analysis. Journal of Neuroscience Methods [Internet]. 2004 Mar [cited 2021 Sep 19]; 134(1):9–21. Available from: https://linkinghub.elsevier.com/retrieve/pii/S0165027003003479. https://doi.org/10.1016/j.jneumeth.2003.10.009 PMID: 15102499

37. Womelsdorf T, Schoffelen JM, Oostenveld R, Singer W, Desimone R, Engel AK, et al. Modulation of Neuronal Interactions Through Neuronal Synchronization. Science [Internet]. 2007 Jun 15 [cited 2021 Nov 4]; 316(5831):1609–12. Available from: https://www.science.org/doi/10.1126/science.1139597. PMID: 17569862

38. Thomson DJ. Spectrum estimation and harmonic analysis. Proceedings of the IEEE. 1982 Sep; 70 (9):1055–96.

39. Mitra PP, Bokil HS. Observed Brain Dynamics [Internet]. Oxford University Press. Oxford University Press; 2007 [cited 2021 Sep 19]. 408 p. Available from: https://global.oup.com/academic/product/observed-brain-dynamics-9780195178081?cc=us&lang=en&.

40. Engel AK, Fries P. Beta-band oscillations—signalling the status quo? Current Opinion in Neurobiology [Internet]. 2010 Apr 1 [cited 2022 May 25]; 20(2):156–65. Available from: https://www.sciencedirect.com/science/article/pii/S0959438810000395. https://doi.org/10.1016/j.conb.2010.02.015 PMID: 20359884

41. Martin Bland J, Altman Douglas G. STATISTICAL METHODS FOR ASSESSING AGREEMENT BETWEEN TWO METHODS OF CLINICAL MEASUREMENT. The Lancet [Internet]. 1986 Feb 8 [cited 2022 Aug 25]; 327(8476):307–10. Available from: https://www.sciencedirect.com/science/article/pii/S0140673686908378.

42. Mann HB, Whitney DR. On a Test of Whether one of Two Random Variables is Stochastically Larger than the Other. Ann Math Statist [Internet]. 1947 Mar [cited 2021 Oct 1]; 18(1):50–60. Available from: http://projecteuclid.org/euclid.aoms/1177730491.

43. Berry KJ, Johnston JE, Mielke PW. Permutation methods: Permutation methods. WIREs Comp Stat [Internet]. 2011 Nov [cited 2021 Oct 1]; 3(6):527–42. Available from: https://onlinelibrary.wiley.com/doi/https://doi.org/10.1002/wics.177

44. Benjamini Y, Hochberg Y. Controlling the False Discovery Rate: A Practical and Powerful Approach to Multiple Testing. Journal of the Royal Statistical Society: Series B (Methodological) [Internet]. 1995 [cited 2021 Oct 27]; 57(1):289–300. Available from: https://onlinelibrary.wiley.com/doi/abs/10.1111/j.2517-6161.1995.tb02031.x.

45. Engbert R. Microsaccades: a microcosm for research on oculomotor control, attention, and visual perception. In: Martinez-Conde S, Macknik SL, Martinez LM, Alonso JM, Tse PU, editors. Progress in Brain Research [Internet]. Elsevier; 2006 [cited 2022 May 25]. p. 177–92. (Visual Perception; vol. 154). Available from: https://www.sciencedirect.com/science/article/pii/S0079612306540099.

46. Debener S, Minow F, Emkes R, Gandras K, de Vos M. How about taking a low-cost, small, and wireless EEG for a walk? Psychophysiology [Internet]. 2012 [cited 2021 Oct 14]; 49(11):1617–21. Available from: https://onlinelibrary.wiley.com/doi/abs/10.1111/j.1469-8986.2012.01471.x. PMID: 23013047

47. Krigolson OE, Williams CC, Norton A, Hassall CD, Colino FL. Choosing MUSE: Validation of a Low-Cost, Portable EEG System for ERP Research. Frontiers in Neuroscience [Internet]. 2017 [cited 2021 Oct 14]; 11:109. Available from: https://www.frontiersin.org/article/10.3389/fnins.2017.00109. https://doi.org/10.3389/fnins.2017.00109 PMID: 28344546

48. Ratti E, Waninger S, Berka C, Ruffini G, Verma A. Comparison of Medical and Consumer Wireless EEG Systems for Use in Clinical Trials. Frontiers in Human Neuroscience [Internet]. 2017 [cited 2021 Oct 14]; 11:398. Available from: https://www.frontiersin.org/article/10.3389/fnhum.2017.00398. https://doi.org/10.3389/fnhum.2017.00398 PMID: 28824402